



Real-time Identification and Measurement of Transmission Lines Based On Mobile LiDAR Scanning

Minglei Li¹  · Li Xu¹ · Min Li¹

Received: 13 November 2024 / Accepted: 1 April 2025

© Deutsche Gesellschaft für Photogrammetrie, Fernerkundung und Geoinformation (DGPF) e.V. 2025

Abstract

Real-time monitoring of the distance between highly mobile equipment and transmission lines is of great significance to ensure the safe maintenance and construction of these infrastructures. We propose a novel identification and measurement technique that utilizes Light Detection and Ranging (LiDAR) scanning to achieve 3D perception. Firstly, a local dense 3D point cloud map is created through a short-term Simultaneous Localization and Mapping (SLAM) method. Then, a deep 3D neural network is implemented by integrating voxel downsampling and spatial distribution features of the transmission lines to improve recognition capabilities. The method employs fast Euclidean distance for instance segmentation, while misclassified points outside the base of transmission towers are eliminated through contour extraction. Experimental results on real datasets validate that our proposed method not only fulfills the real-time measurement requirements but also surpasses the performance of existing algorithms.

Keywords Transmission line · LiDAR · Deep 3D neural network · Point cloud segmentation · Distance measurement

1 Introduction

The live maintenance of transmission lines is crucial for the stable operation of the power grid. This allows activities to be carried out without interrupting the power supply, minimizing downtime. However, there is currently a lack of effective methods for real-time monitoring of the safety distance between workers/equipment and surrounding transmission lines during live maintenance (Shokri et al. 2021; Zeng et al. 2010). Traditional power engineering measurements are based on human visual inspection, which is dangerous and inefficient. Transmission lines are mainly made up of latticed towers and slender power lines, which can cause workers to make misjudgments in conditions of strong or insufficient light (Li and Zhang 2016). Therefore,

accurately measuring the distance at the operation sites in real-time remains a challenge.

Visual images have been used for the design of intelligent distance measurement methods, using monocular (Cheng and Wu 2019) or binocular (Huang et al. 2020; Ma et al. 2021) cameras. By extracting feature points and performing triangulation between views, 3D models are recovered and the distances between equipment and transmission lines are measured. However, transmission lines exhibit long spans and often lack sufficient distinguishing features, which can result in repeated similar images, leading to mismatches between different views.

Light Detection and Ranging (LiDAR) scanning technology provides a 3D measurement method distinct from visible light images, with strong adaptability to various lighting conditions. In recent years, LiDAR devices have been widely used in transmission line measurements. However, the automatic extraction of object-level information from 3D point cloud data in real-time for transmission lines still faces some challenges (Chen et al. 2022).

Early techniques for segmenting transmission lines from LiDAR point clouds relied on fitting models that leveraged the spatial distribution characteristics of these lines, such as height and point density. Once these towers are located, the 3D point clouds are converted into 2D grids or projected images. Subsequent extraction of power lines from

✉ Minglei Li
minglei_li@nuaa.edu.cn

Li Xu
sz2204056@nuaa.edu.cn

Min Li
sx2304080@nuaa.edu.cn

¹ College of Electronic and Information Engineering, Nanjing University of Aeronautics and Astronautics, 211106 Nanjing, China

these 2D representations often utilized techniques such as the Hough Transform (HT) or Random Sample Consensus (RANSAC) (Yadav and Chousalkar 2017). After extraction, power lines were typically modeled with parameterized geometric models to represent their physical curvature (Zhang et al. 2019). These methods underscore the complexities involved in effectively segmenting and analyzing transmission line structures within point clouds.

Alternative methods for segmenting and extracting point clouds in 3D employ techniques such as Euclidean clustering or region growing based on some morphology-based strategies. (Ni et al. 2017). However, morphological methods require complex mathematical modeling that accounts for the spatial distribution characteristics of transmission lines. They are typically more effective in flatter landscapes with minimal tree coverage and reduced environmental fluctuations. Some researchers have sought to develop geometric features for transmission lines and employ machine learning classifiers, including Support Vector Machines (SVM), Random Forests, and JointBoost (Guo et al. 2015; Kim and Sohn 2012; Wang et al. 2017), to achieve good segmentation results.

The rise of deep learning has led researchers to explore its application in segmenting objects in point clouds (Kumar et al. 2024). tested mainstream deep learning algorithms such as KPConv (Thomas et al. 2019), PointCNN (Shi et al. 2019), and RandLA-Net (Hu et al. 2020) on transmission line point cloud datasets, and the results showed that these algorithms perform well in classifying power line points, surpassing traditional methods. Furthermore, (Li et al. 2024) proposed an improved PointNet++ algorithm (Qi et al. 2017b) tailored to the characteristics of transmission line point clouds, where the target structures are large, but the proportion of point cloud data is small. They modified the set abstraction module of the PointNet++ (Qi et al. 2017b) algorithm to better adapt to transmission lines, using h-Swish as the activation function to achieve a precise classification of features in transmission lines. Current deep learning-based algorithms for the recognition of transmission lines utilizing 3D data are primarily post-processing techniques applied to offline point cloud datasets, which presents significant limitations in meeting real-time distance measurement requirements.

This paper proposes a method that integrates a Simultaneous Localization and Mapping (SLAM) technique with a deep learning network to generate real-time processing capabilities in dynamic environments. LiDAR-based SLAM technology can unify the coordinate system of the point cloud for the entire observation scene, enabling fast and precise multi-frame registration. This technology has garnered extensive research and application in various domains, including autonomous driving and remote sensing (Bresson et al. 2017; Stefano et al. 2021).

Considering the sparsity of single-frame point clouds in transmission line environments, we propose a local mapping mechanism utilizing a short-term LiDAR SLAM algorithm. In addition, we introduce a deep 3D neural network called PowerLine-Net, which extracts spatial distribution features and incorporates them into the classification module for transmission line recognition. PowerLine-Net enables more accurate segmentation of transmission lines from point clouds and significantly enhances accuracy across various environments.

2 Methods

The workflow of the proposed method is shown in Fig. 1, mainly including a short-term SLAM module, a deep neural network classification module, and an instance segmentation and ranging module. The method can efficiently and accurately extract the point clouds of transmission lines from dynamic mobile LiDAR scanning and measure their relative distances.

2.1 Dynamic Local Mapping

Transmission lines, characterized by their multi-strand catenary structures, pose challenges for capturing their complete shape from a single LiDAR point cloud frame because of the potential for data omission arising from their slender nature. This study proposes a methodology for dynamically generating local maps of the observation area by aggregating multiple scanning frames.

Most classic SLAM algorithms follow an incremental mapping scheme, resulting in a continuous increase in data volume over time. However, in the context of real-time measurements of object instances, a local map around the measuring equipment is enough to complete the required monitoring task. Therefore, we first use a short-term SLAM method modified on the Fast-LIO2 algorithm (Xu et al. 2022) to perform multi-frame point cloud registration and generate a dynamic local map, thereby achieving a dense point cloud. Then, PowerLine-Net is used on the local map to realize the identification and measurement of transmission lines.

The Fast-LIO2 algorithm (Xu et al. 2022) is an inertial odometry method that tightly integrates iterative Kalman filtering with datasets from LiDAR and Inertial Measurement Units (IMU). Specifically, the algorithm utilizes IMU data to propagate the LiDAR information forward, thereby reducing errors caused by motion. Subsequently, these IMU data are used to construct the state transition equation, enabling the calculation of state errors at each time step. The discrepancy between the current point cloud frame and a pre-existing 3D map is regarded as the observation error,

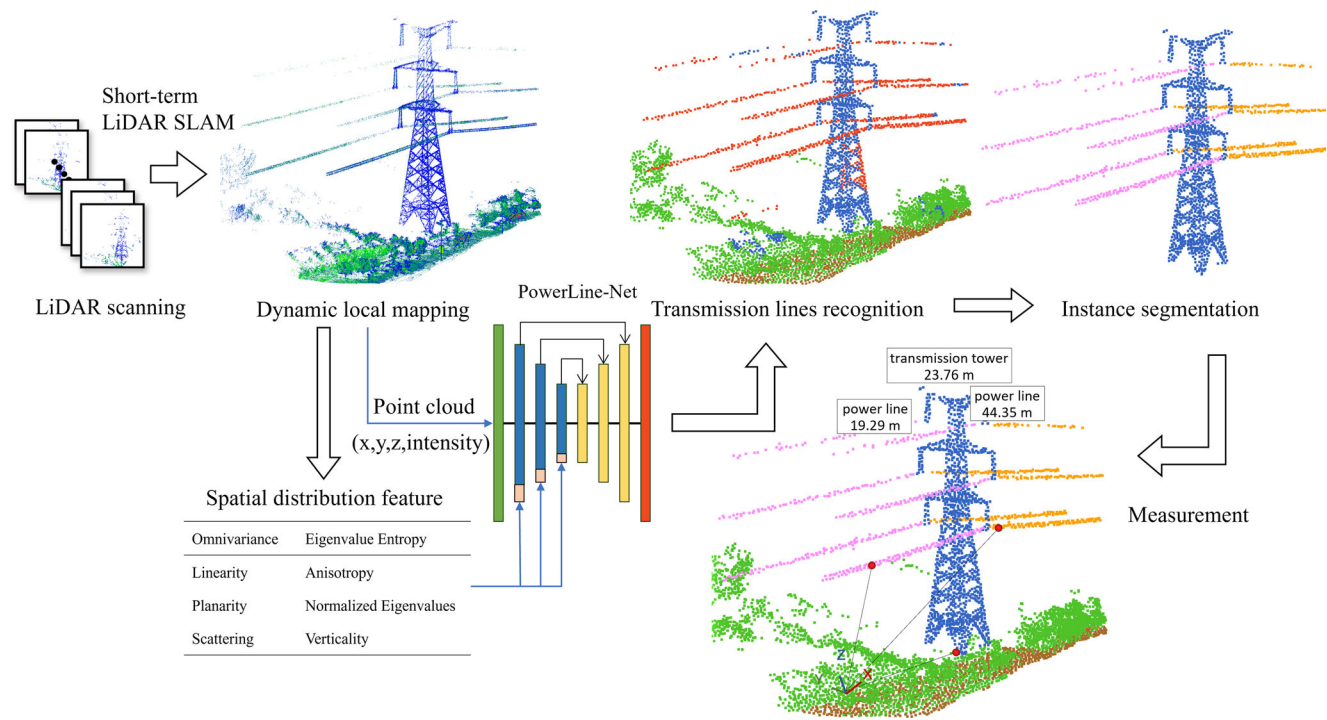


Fig. 1 The real-time measurement workflow for transmission lines

which forms a maximum a posteriori (MAP) estimation framework. By incorporating Kalman gain, the framework allows for iterative refinement until a convergence criterion is satisfied, resulting in globally optimal estimates for the registration parameters of the current frame.

To tackle the issue of incremental expansion of the 3D map, we designed a sliding spatial window to effectively manage the local map zone by eliminating points situated a considerable distance from the observation center. A schematic representation of the dynamic enhancement process of the local map is illustrated in Fig. 2. This process incorporates two critical distance thresholds, r and l , with the condition that $r > l$. These thresholds delineate the distance limit for the area of interest and the offset distance limit for the LiDAR scan center, respectively. Points C and C' represent the positions of the previous and current real-time LiDAR scan centers. When the offset of the scan center surpasses the threshold l , the coordinates of the current scan center are designated as a new reference point, leading to the generation of an incremental 3D point cloud map within a radius of r from that reference point.

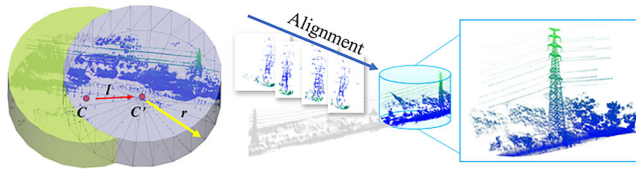


Fig. 2 Schematic of the dynamic local mapping method

2.2 Semantic Segmentation

Accurate recognition of transmission lines in real-time requires fast and precise segmentation of the 3D point cloud. We propose a PowerLine-Net that is capable of segmenting transmission lines within extensive scenes, by integrating spatial distribution characteristics pertinent to transmission line targets.

To generate subset features as an approximate representation of the original point cloud, traditional deep learning for point cloud segmentation usually employs farthest point sampling or inverse density importance sampling (IDIS), with time complexities of $O(N^2)$ and $O(N)$, respectively. In contrast, random sampling (RS) used in RandLA-Net (Hu et al. 2020) has a time complexity of $O(1)$, making it more efficient. However, in the context of transmission line point cloud scenarios characterized by uneven density distributions, RS may lead to the generation of unstable learned features, particularly in areas with a scarcity of key features. This instability can adversely affect the performance of the model. Furthermore, RS does not guarantee uniform coverage throughout the space, which can result in inadequate learning in certain local regions, which in turn compromises the model's comprehension of the global scene (Lyu et al. 2024). To address these limitations, we propose substituting RS with voxel downsampling (VS), a method that partitions the space into uniform cubic grids and selects the point closest to the grid center as the repre-

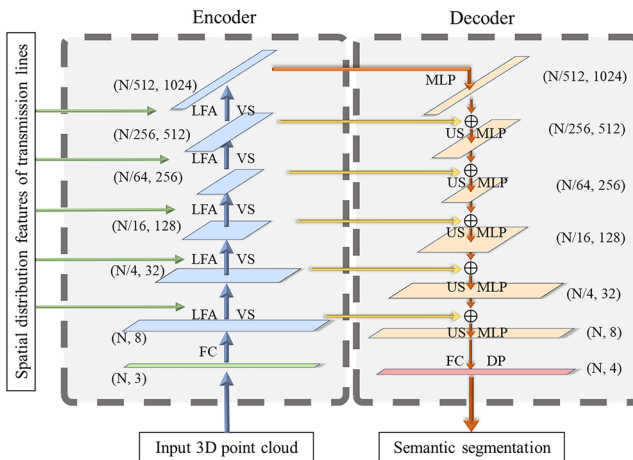


Fig. 3 Architecture of PowerLine-Net. ((*N*, *D*) Dimensions of points and features, *FC* Full convolution, *LFA* Local feature aggregation, *VS* Voxel down-sampling, *MLP* Multi-layer perception, *US* Up sampling, *DP* Dropout)

sentative point. The proposed 3D neural network structure is shown in Fig. 3.

As transmission lines have a large spatial span and more isolated points, the spatial distribution of their point clouds serves as a highly discriminative characteristic. Earlier machine learning classifiers for transmission line point clouds commonly rely on manually designed features, including local neighborhood characteristics, point density, and vertical distribution, forming a feature space for classification (Wang et al. 2018). The discriminative power of features is closely related to the classification accuracy of machine learning algorithms. Thus, we incorporate these manual features into our network as training parameters. The spatial distribution features are computed by calculating the covariance matrix of the neighborhood points within a distance *l* from the center point, and then solving for the eigenvalues $\lambda_1, \lambda_2, \text{ and } \lambda_3$ ($\lambda_1 > \lambda_2 > \lambda_3$) and their corresponding eigenvectors $v_1, v_2, \text{ and } v_3$. The detailed calculation of spatial distribution features is shown in Table 1.

The spatial distribution features in Table 1 are carefully selected and have a strong discrimination ability for different targets in the point cloud of the transmission line. For example, omnivariance (OV) reflects the geometric shape

complexity of the point cloud in the local area. If the OV value is large, it indicates that the point cloud distribution in this local area is relatively scattered, and the geometric structure is complex, where there may be trees or more irregular shapes. In contrast, a smaller OV value means that the point cloud distribution in the local area is relatively concentrated, and the geometric structure is simple, which may be power lines, the ground, or regular geometric shapes. Another example is that when the points in the point cloud neighborhood are significantly arranged along a certain principal direction, it shows strong linearity (LI), which is common in power line point clouds.

The local feature aggregation (LFA) module explicitly encodes the 3D coordinates of input point clouds, allowing each center point p_i to contain information about its surrounding *K* points $\{p_i^1, p_i^2, \dots, p_i^k, \dots, p_i^K\}$. This improves the aggregation of features from the spatial shape of the point cloud. As a result, the network can better learn the geometric structure of space from the relative positions and distance information of individual points. In RandLA-Net, the local encoding information comprises the 3D coordinates p_i of the central point, the 3D coordinates p_i^k of the neighboring points, the relative coordinates $(p_i - p_i^k)$ between the central point and its neighbors, as well as the Euclidean distance $\|p_i - p_i^k\|$ between the central point and the neighboring points. In contrast, this paper introduces an enhancement in which the spatial distribution features F_i^k of the neighboring points are integrated into the encoding process. The formula for the revised local spatial encoding r_i^k is expressed as follows:

$$r_i^k = \text{MLP}(p_i \oplus p_i^k \oplus (p_i - p_i^k) \oplus \|p_i - p_i^k\| \oplus F_i^k)$$

In the formula, \oplus denotes feature concatenation. Using a shared multi-layer perceptron (MLP) with learnable parameters, the learned attention scores are treated as a flexible mask that automatically selects important features, producing weighted sums of the neighborhood point sets. This enhances the aggregation of neighborhood point feature sets, preventing the loss of important points during VS processing.

Table 1 The calculation of spatial distribution features

Feature Category	Feature Name	Abbreviation	Calculation
Geometric features	Eigenvalue Entropy	EE	$-\sum_{i=1}^3 \frac{\lambda_i}{\sum \lambda_i} \ln(\frac{\lambda_i}{\sum \lambda_i})$
	Omnivariance	OV	$\sqrt[3]{\lambda_1 \lambda_2 \lambda_3}$
Distributional features	Linearity	LI	$(\lambda_1 - \lambda_2)/\lambda_1$
	Planarity	PL	$(\lambda_2 - \lambda_3)/\lambda_1$
	Scattering	SP	λ_3/λ_1
	Anisotropy	AS	$(\lambda_1 - \lambda_3)/\lambda_1$
	Normalized Eigenvalues	NE	$\lambda_3 / \sum_{i=1}^3 \lambda_i$
	Verticality	VE	$v_{13} / \ v_1\ $

2.3 Instance Segmentation

The PowerLine-Net involves the segmentation of locally reconstructed maps into semantic categories, including power lines, towers, ground, and others. Nonetheless, the outcomes of semantic segmentation are often compromised by discrete noise and misclassified points, which can be attributed to hardware constraints. Additionally, the presence of intricate scenes featuring multiple transmission towers and power lines necessitates further instance segmentation to accurately calculate distances to each individual object. In practice, it is common for transmission towers to be erected at predetermined intervals. Hence, we employ a rapid Euclidean clustering technique (Cao et al. 2022) to effectively segment the point clouds associated with power lines and transmission towers into distinct instances, while simultaneously filtering out misclassified points.

During the recognition of transmission lines, misclassified points from vegetation and ground around the transmission tower may be grouped as part of the tower, connecting misclassified points to the tower and causing deviations in distance measurement results. This issue mainly arises at the bases of the towers. Transmission towers are generally vertical to the ground, meaning the Z-axis is perpendicular to the X-Y plane. To take advantage of the tower's symmetry, we rotate the transmission tower point cloud around the Z-axis by θ degrees to align the tower's arms parallel to the Y-axis. We apply Principal Component Analysis (PCA) to compute the eigenvalues and eigenvectors of the tower point cloud. The eigenvector v corresponding to the smallest eigenvalue is selected as the new X'-axis, and the tower point cloud is rotated accordingly.

Since the base of the tower is typically a quadrilateral frustum, the height of the tower and its projection length in the Y'-Z plane have a linear relationship (Chen et al. 2014). We slice the transmission tower along the Z-axis, setting the slice interval to Δh , and project each slice's point cloud in the Y' direction. For each slice, we select the maximum and minimum points on the X'-axis to calculate the 2D projection contour points of the tower. Denoting the current slice index as i , we calculate the slope of the contour points in the neighborhood $[i-2, i+2]$, and the last significant slope change is marked as the boundary between the lower and upper parts of the tower. We use the RANSAC algorithm to extract the line formed by the contour points, representing the lower contour line of the transmission tower. Points outside the contour line are filtered out, and the remaining points are restored to 3D space. The same process is applied to the projection in the X'-Z plane to remove misclassified points on the outside of the lower part of the tower. Figure 4 shows an example of the process for removing misclassified points at the tower base.

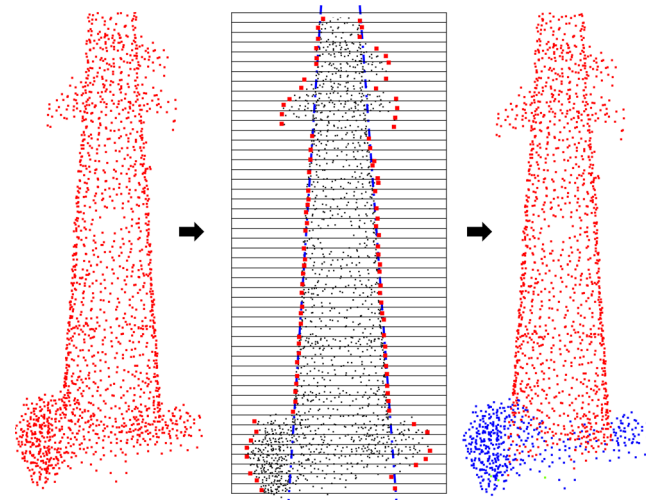


Fig. 4 An illustration of removing misclassified points

3 Experiments and Results

3.1 Experiment Setup

The experimental platform for training the proposed PowerLine-Net is detailed in Table 2.

The experiments used 3D point cloud data obtained from three transmission lines with different voltage levels in Nanjing, China, to validate the proposed method. The collection locations include urban, suburban, and multi-line intersection areas. The study area consists of complex scenes with densely distributed high-rise buildings in the city center, regions with rich vegetation in the suburbs, and specific locations where multiple transmission lines run in parallel. The transmission towers involved vary in type, covering multiple structural forms, and include transmission lines of different voltage levels. The dataset includes 28 transmission towers with different shapes and 19 power lines, thus providing a rich set of sample data for the research.

These datasets were collected using a handheld Livox AVIA LiDAR integrated with an NVIDIA Jetson Orin Nano board. The composition of the system is shown in Fig. 5.

The full views of three survey areas are shown in Fig. 6, where the color of the point clouds is rendered as a pseudo-color image based on height.

Table 2 PowerLine-Net training platform

Component	Configuration
CPU	Intel® Core™ i7-12700 @ 2.10GHz
GPU	NVIDIA GeForce GTX 3060 12 GB
RAM	64 GB
System	Ubuntu 20.04 LTS
Language	C++, Python

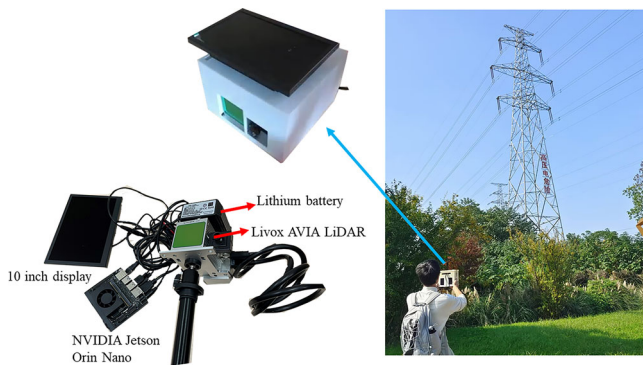


Fig. 5 The composition of the LiDAR scanning system

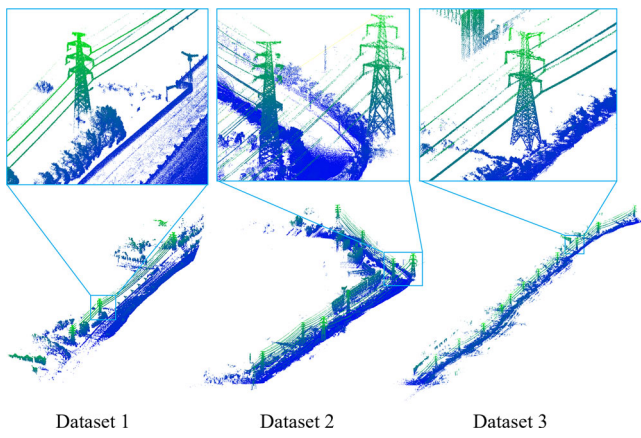


Fig. 6 three sets of experimental data, color indicate height

Table 3 Detailed information on the three datasets collected

Information	Dataset 1	Dataset 2	Dataset 3
Voltage (kV)	220	110	500
Length (km)	1.1	0.4	3.4
Number (Million)	8.79	5.69	33.29

Detailed information about the datasets is shown in Table 3.

3.2 Qualitative Analysis

Taking Dataset 1 as an example, we calculate the spatial distribution features of the transmission line are calculated, and the rendered images of these features are shown in Fig. 7. Fig. 7 utilizes pseudo-color rendering to visualize the normalized results presented in Table 1. The computed values are scaled from 0 to 1 and are represented with a gradient color scheme, blue>green> yellow>red. It can be observed that the spatial distribution features of the point cloud have different reflections on power lines, transmission towers, ground, and background objects to a certain extent. Therefore, by integrating these features into the encoder of

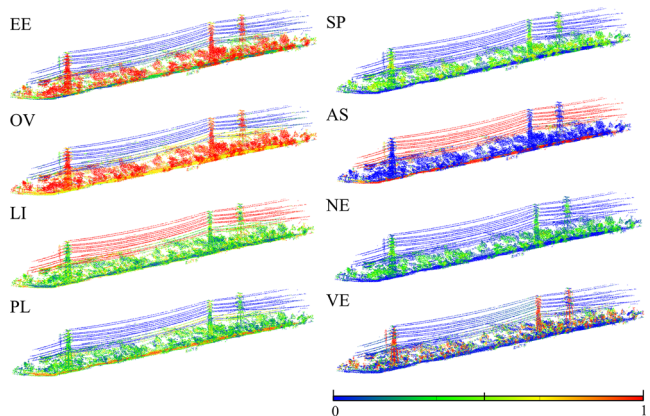


Fig. 7 Visualization of spatial distribution features of transmission lines

the deep network, the discriminative performance of deep features can be effectively improved.

We used annotation software to manually annotate the generated local point cloud maps frame by frame. The annotations cover four categories: transmission towers, power lines, the ground, and others. Moreover, according to the chronological order of point cloud data collection in each of the three datasets, we divided the data into a training set, a validation set, and a test set at a ratio of 6:2:2. This approach avoids data overlap and ensures the independence of data distribution in the validation and test sets, thereby enhancing the accuracy of model evaluation and the generalization ability of the model.

Using the proposed PowerLine-Net, semantic segmentation is performed on datasets. The segmentation results are shown in Fig. 8, where the red points represent power lines, the green points represent transmission towers, the yellow points represent ground, and the blue points represent other points. The figure shows that each object in the scene is segmented with relative accuracy.

3.3 Quantitative Analysis

To evaluate the accuracy of the distance measurement, we selected several target points within the datasets, comparing the true distances with the measurement results. The distance measurement statistic is shown in Table 4.

The results of the quantitative experiments demonstrate that the proposed method for measuring the distance of transmission line targets exhibits good performance. Furthermore, the proposed method performs well across three different datasets, each containing variations in terrain, point density, transmission tower types, and voltage levels.

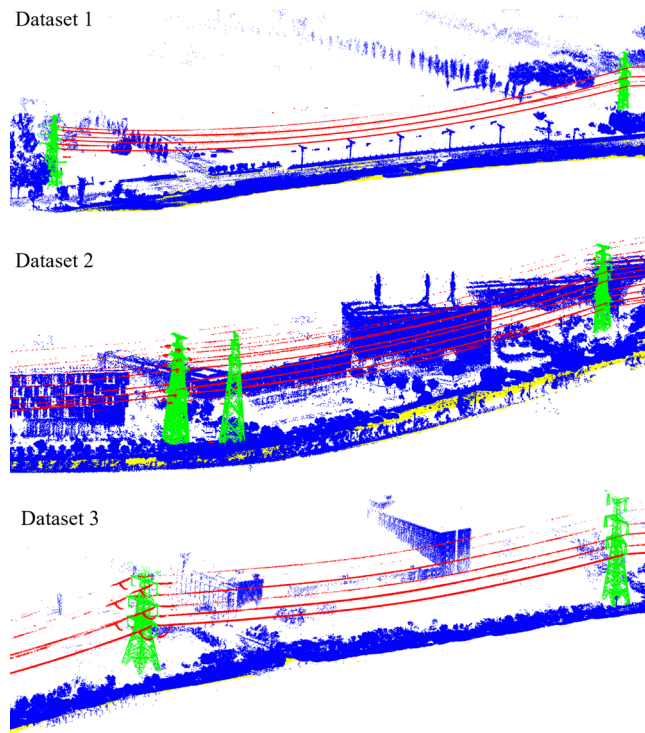


Fig. 8 Visual results of the point cloud classification

3.4 Comparative Analysis

We conducted a comparative evaluation of the proposed method with state-of-the-art algorithms, including PointNet (Qi et al. 2017a), PointNet++ based method (Li et al. 2024), KPConv based method (Kumar et al. 2024), and RandLA-Net based method (Hu et al. 2020) in terms of localization accuracy and recognition performance. The visual comparative results are shown in Fig. 9.

PointNet (Qi et al. 2017a) processes the global point cloud in a manner that neglects local structural information, which can hinder its ability to adequately capture local geometric features in intricate scenes, particularly at the intersections of power lines and transmission towers,

where a significant number of misclassified points are observed. PointNet++ based method (Li et al. 2024) endeavors to address this issue by employing a hierarchical approach to capture local features, demonstrating enhanced sensitivity to the local characteristics of transmission lines. However, its grouping strategy and feature extraction techniques exhibit suboptimal performance when confronted with the non-uniformly sampled raw point clouds of transmission lines, thereby diminishing the accuracy of local feature extraction. KPConv based method (Kumar et al. 2024) employs variable convolution kernels to address the challenges associated with variations in point cloud density during sampling. Nevertheless, its dependence on local information through attention mechanisms may lead to a loss of global structural information or an inadequate comprehension of the overall scene. The local aggregation module of the RandLA-Net based method (Hu et al. 2020) alleviates some of the uncertainties arising from fluctuations in point cloud density. However, it encounters difficulties in accurately segmenting points in proximity to trees and buildings due to the selection of imprecise points during the neighborhood aggregation process. To further mitigate the adverse effects of point cloud density, our approach employs voxel downsampling. Although it sacrifices some computational speed, it yields better results. Moreover, integrating the spatial distribution features of transmission lines and contour extraction based on the morphological features of transmission towers enhances recognition accuracy and eliminates misidentified points at the bottom of transmission towers.

This paper utilizes overall accuracy (OA) as the evaluation metric for recognition accuracy, while also employing mean absolute error (MAE) and frames per second (FPS) to quantify the precision and speed of distance measurement.

$$OA = \frac{TP}{M}$$

$$MAE = \frac{1}{n} \sum_{i=1}^n |D_i - \hat{D}_i|$$

Table 4 Measurement record of transmission line objects

Object	Transmission tower					Power line						
	0	3	6	9	12	15	0	3	6	9	12	15
ID	9.04	54.44	111.31	105.72	61.38	23.76	20.68	19.65	18.50	16.77	18.67	19.29
Measure distance (m)	20.48	76.87	123.02	91.45	46.3	12.45	20.75	19.27	18.73	17.46	18.84	19.25
	35.87	96.16	115.48	76.41	35.42	5.8	20.38	18.99	17.75	17.87	19.55	19.27
Actual distance (m)	8.95	54.21	110.12	105.42	61.74	23.59	20.84	19.89	18.72	16.59	18.45	19.55
	20.34	76.65	121.84	91.21	46.48	12.34	20.56	19.50	18.33	17.21	19.07	19.48
	35.78	95.89	115.64	76.65	35.21	5.61	20.28	19.11	17.94	17.83	19.39	19.41
Error distance (m)	0.09	0.23	1.19	0.30	-0.36	0.17	-0.16	-0.24	-0.22	0.18	0.22	-0.26
	0.14	0.22	1.18	0.24	-0.18	0.11	0.19	-0.23	0.40	0.25	-0.23	-0.23
	0.09	0.27	-0.16	-0.24	0.21	0.19	0.10	-0.12	-0.19	0.04	0.16	-0.14

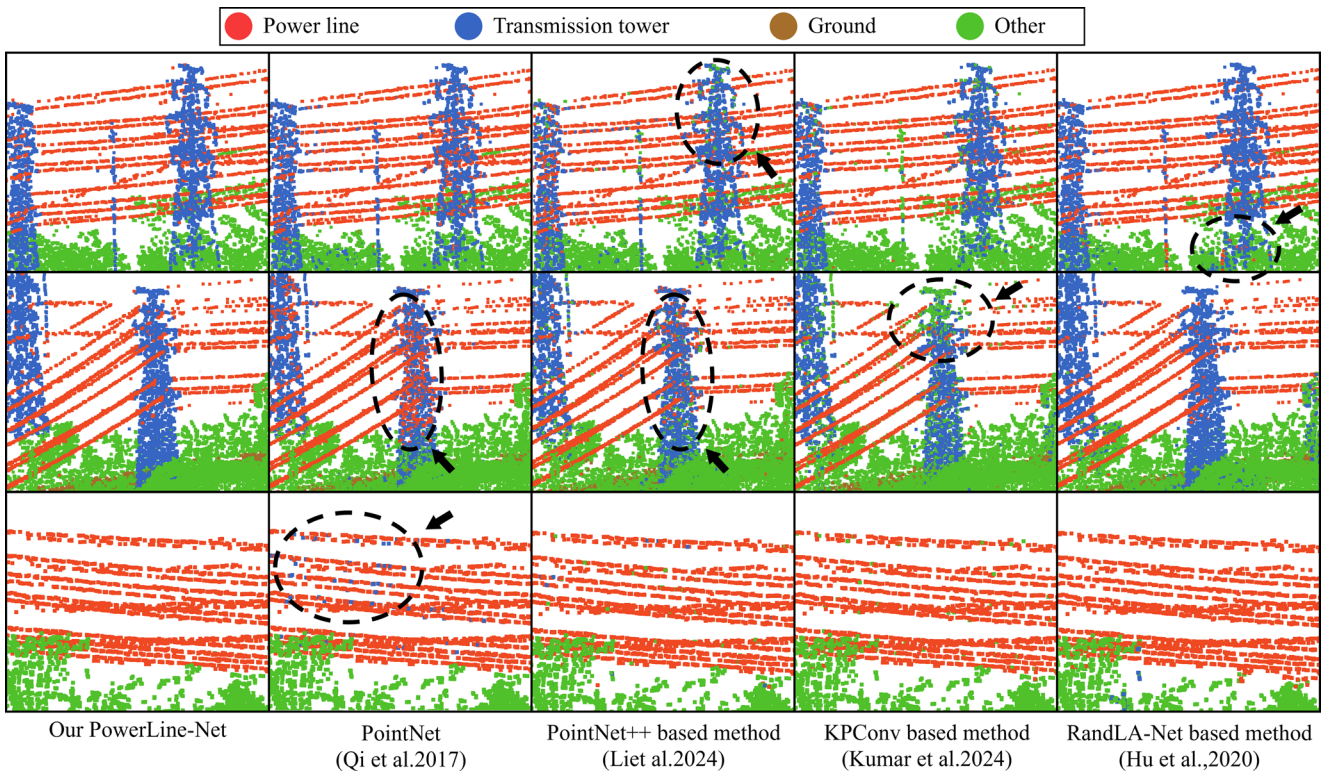


Fig. 9 Comparison of recognition results of different algorithms

TP means a number of true-positive points, *M* means a total number of points, *n* is the number of frames, D_i and \hat{D}_i represent the actual and predicted distance between LiDAR and transmission line objects. The quantitative analysis results of the different algorithms are summarized in Table 5. The proposed algorithm attains an OA of 95.3%, which is higher than that of other methods. This finding further substantiates the precision and dependability of our approach in identifying transmission line targets. Furthermore, the mean absolute error (MAE) between the measured distance and the actual distance is recorded at 0.25 m, which is less than that observed in the other methods. This low MAE value indicates that our method has high accuracy in distance measurement. Such high-accuracy distance measurement is of great significance for practical applications in the construction and maintenance of transmission lines. It can provide more reliable data support and help prevent

safety accidents caused by power transmission to personnel and equipment.

Although PointNet (Qi et al. 2017a) is capable of processing global point clouds at a faster rate, its detection accuracy is inferior to that of our method and the RandLA-Net based algorithm (Hu et al. 2020). While PointNet++ based method (Li et al. 2024) extracts local features hierarchically, it increases computational complexity, resulting in lower efficiency during training and inference, especially when processing large-scale point clouds. Likewise, KPConv based method (Kumar et al. 2024) uses multiple convolution kernels within the local neighborhood of each point to capture geometric features demands substantial computational resources. In contrast, our method demonstrates superior performance in real-time operations.

The remarkable segmentation performance of the PowerLine-Net proposed in this paper can be attributed to two main factors. Firstly, it is specifically designed for large-scale point cloud data of transmission lines. During training, it integrates the spatial distribution features of transmission lines and uses voxel downsampling instead of random downsampling to enhance recognition accuracy and robustness. Secondly, in the instance segmentation and contour extraction stages, misclassified point clouds in transmission lines are further removed, especially the interference points at the intersections of transmission tower bodies with surrounding trees and the ground, as well as the discrete points

Table 5 Quantitative analysis of different algorithms

Algorithm	OA/%	MAE/m	FPS/Hz
PointNet (Qi et al. 2017a)	87.9	0.85	3.3
PointNet++ (Li et al. 2024)	88.9	0.52	1.5
KPConv (Kumar et al. 2024)	92.0	0.40	2.7
RandLA-Net (Hu et al. 2020)	91.5	0.33	3.2
Ours	95.3	0.25	3.0

between power lines, thus improving the accuracy of distance measurement.

4 Conclusions

This paper presents a real-time identification and measurement method for the monitoring of transmission lines based on LiDAR scanning. The method uses a short-term SLAM technique to dynamically generate local 3D maps. Additionally, a deep 3D neural network is used to segment objects within the local map, and misclassified points are removed using shape characteristics. Finally, real-time measurements are taken on different object instances. The experimental results on three real-world datasets, as well as comparisons with other methods, have validated the effectiveness of the proposed method.

Funding This work was funded in part by the National Natural Science Foundation of China (Grant No. 42271343) and the Open Project Funds for the Joint Laboratory of Spatial Intelligent Perception and Large Model Application (Grant No. SIPLMA-2024-YB-06).

Declarations

Conflict of interest M. Li, L. Xu and M. Li declare that they have no competing interests.

Ethical standards For this article no studies with human participants or animals were performed by any of the authors. All studies mentioned were in accordance with the ethical standards indicated in each case.

References

- Bresson G, Alsayed Z, Yu L et al (2017) Simultaneous localization and mapping: A survey of current trends in autonomous driving. *IEEE Trans Intell Veh* 2(3):194–220. <https://doi.org/10.1109/TIV.2017.2749181>
- Cao Y, Wang YC, Xue YF et al (2022) Fec: fast euclidean clustering for point cloud segmentation. *Drones* 6(11):325. <https://doi.org/10.3390/drones6110325>
- Chen C, Jin A, Yang BS et al (2022) Dcpd-net: a diffusion coupled convolution neural network for real-time power transmission lines detection from uav-borne lidar data. *Int J Appl Earth Obs Geoinform* 112:102960. <https://doi.org/10.1016/j.jag.2022.102960>
- Chen ZP, Lan ZR, Long HP et al (2014) 3d modeling of pylon from airborne lidar data. In: 2014 remote sensing of the environment: 18th national symposium on remote sensing of China SPIE. vol 9158, pp 29–36 <https://doi.org/10.1117/12.2063873>
- Cheng L, Wu GP (2019) Obstacles detection and depth estimation from monocular vision for inspection robot of high voltage transmission line. *Cluster Comput* 22(Suppl 2):2611–2627. <https://doi.org/10.1007/s10586-017-1356-8>
- Di Stefano F, Chiappini S, Gorreja A et al (2021) Mobile 3d scan lidar: a literature review. *Geom Nat Hazards Risk* 12(1):2387–2429. <https://doi.org/10.1080/19475705.2021.1964617>
- Guo B, Huang XF, Zhang F et al (2015) Classification of airborne laser scanning data using jointboost. *ISPRS J Photogramm Remote Sens* 100:71–83. <https://doi.org/10.1016/j.isprsjprs.2014.04.015>
- Hu QY, Yang B, Xie LH et al (2020) Randla-net: Efficient semantic segmentation of large-scale point clouds. In: 2020 Proceedings of the IEEE/CVF conference on computer vision and pattern recognition (CVPR), pp 11108–11117 <https://doi.org/10.1109/cvpr42600.2020.01112>
- Huang L, Wu GP, Liu JY et al (2020) Obstacle distance measurement based on binocular vision for high-voltage transmission lines using a cable inspection robot. *Sci Prog* 103(3):36850420936910. <https://doi.org/10.1177/0036850420936910>
- Kim HB, Sohn G (2012) Random forests based multiple classifier system for power-line scene classification. *Int Arch Photogramm Remote Sens Spatial Inf Sci* 38:253–258. <https://doi.org/10.5194/isprarchives-XXXVIII-5-W12-253-2011>
- Kumar V, Nandy A, Soni V et al (2024) Powerline extraction from aerial and mobile lidar data using deep learning. *Earth Sci Inform.* <https://doi.org/10.1007/s12145-024-01310-w>
- Li B, Liu SY, Wang XF et al (2024) A classification model for power corridors based on the improved pointnet++ network. *Geocarto Int* 39(1):2297556. <https://doi.org/10.1080/10106049.2023.2297556>
- Li GX, Zhang JX (2016) 3d power line reconstruction from airborne lidar point cloud of overhead electric power transmission corridors. *Acta Geod Cartogr Sinica* 45(3):347. <https://doi.org/10.11947/j.AGCS.2016.20150186>
- Lyu WQ, Ke W, Sheng H et al (2024) Dynamic downsampling algorithm for 3d point cloud map based on voxel filtering. *Appl Sci* 14(8):3160. <https://doi.org/10.3390/app14083160>
- Ma YP, Li QW, Chu LL et al (2021) Real-time detection and spatial localization of insulators for uav inspection based on binocular stereo vision. *Remote Sens* 13(2):230. <https://doi.org/10.3390/rs13020230>
- Ni H, Lin XG, Zhang JX (2017) Classification of als point cloud with improved point cloud segmentation and random forests. *Remote Sens* 9(3):288. <https://doi.org/10.3390/rs9030288>
- Qi CR, Su H, Mo K et al (2017a) Pointnet: Deep learning on point sets for 3d classification and segmentation. In: 2017 Proceedings of the IEEE conference on computer vision and pattern recognition (CVPR), pp 652–660 <https://doi.org/10.1109/cvpr.2017.16>
- Qi CR, Yi L, Su H et al (2017b) Pointnet++: Deep hierarchical feature learning on point sets in a metric space. *Adv Neural Inf Process Syst.* <https://doi.org/10.20944/preprints202403.0743.v1>
- Shi SS, Wang XG, Li HS (2019) Pointrcnn: 3d object proposal generation and detection from point cloud. In: 2019 Proceedings of the IEEE/CVF conference on computer vision and pattern recognition (CVPR), pp 770–779 <https://doi.org/10.1109/cvpr.2019.00086>
- Shokri D, Rastiveis H, Sarasua WA et al (2021) A robust and efficient method for power lines extraction from mobile lidar point clouds. *J Photogramm Remote Sens Geoinformation Sci* 89(3):209–232. <https://doi.org/10.1007/s41064-021-00155-y>
- Thomas H, Qi CR, Deschaud JE et al (2019) Kpconv: Flexible and deformable convolution for point clouds. In: 2019 Proceedings of the IEEE/CVF international conference on computer vision (ICCV), pp 6411–6420 <https://doi.org/10.1109/iccv.2019.00651>
- Wang YJ, Chen Q, Liu L et al (2017) Supervised classification of power lines from airborne lidar data in urban areas. *Remote Sens* 9(8):771. <https://doi.org/10.3390/rs9080771>
- Wang YJ, Chen Q, Liu L et al (2018) Systematic comparison of power line classification methods from als and mls point cloud data. *Remote Sens* 10(8):1222. <https://doi.org/10.3390/rs10081222>
- Xu W, Cai YX, He DJ et al (2022) Fast-lio2: fast direct lidar-inertial odometry. *IEEE Trans Robotics* 38(4):2053–2073. <https://doi.org/10.2139/ssrn.4675561>
- Yadav M, Chousalkar CG (2017) Extraction of power lines using mobile lidar data of roadway environment. *Remote Sens Appl Soc Environ* 8:258–265. <https://doi.org/10.1016/j.rsase.2017.10.007>

- Zeng S, Powers JR, Newbraugh BH (2010) Effectiveness of a worker-worn electric-field sensor to detect power-line proximity and electrical-contact. *J Safety Res* 41(3):229–239. <https://doi.org/10.1016/j.jsr.2010.02.011>
- Zhang RZ, Yang BS, Xiao W et al (2019) Automatic extraction of high-voltage power transmission objects from uav lidar point clouds. *Remote Sens* 11(22):2600. <https://doi.org/10.3390/rs11222600>

Springer Nature or its licensor (e.g. a society or other partner) holds exclusive rights to this article under a publishing agreement with the author(s) or other rightsholder(s); author self-archiving of the accepted manuscript version of this article is solely governed by the terms of such publishing agreement and applicable law.